Prediction of Quadrotor Acoustics Using RVLT Toolchain

Sesi Kottapalli *
Aeromechanics Office
NASA Ames Research Center
Moffett Field, CA, USA

Christopher Silva
Aeromechanics Office
NASA Ames Research Center
Moffett Field, CA, USA

ABSTRACT

The NASA Revolutionary Vertical Lift Technology (RVLT) Project toolchain is used to predict the acoustics of the NASA 6-passenger quadrotor concept vehicle. A qualitative study of the blade vertical loading to understand noise trends with tip speed and number of blades was performed. Trends of the individual rotor noise sources (thickness, loading, and broadband) are studied. Noise is predicted and analyzed for three flight conditions: approach (6-deg descent), level flight flyover, and takeoff. Three quadrotor designs are considered: tip speed=700 ft/sec, 3 blades ("700/3"), "550/3", and "375/7". The qualitative study shows that during approach multiple, strong BVIs occur on the advancing and retreating sides for "700/3" and "550/3", but for "375/7" only weak BVIs are present. Consistent with this BVI scenario, the quadrotor noise results show that "700/3" has the highest loading noise (and EPNL) and "375/7" the lowest loading noise (and EPNL), with "550/3" falling in between. Broadband noise during approach and flyover is roughly the same for all three designs. Takeoff broadband noise is much lower, especially for "375/7". The bulk of the results have been obtained with a rigid uniform blade model, with a flap hinge and a pitch bearing. For "550/3", noise predictions with elastic nonuniform blades have been initiated and are ongoing.

NOTATION

AARON	ANOPP2's Aeroacoustic ROtor **N**oise tool
ANOPP2	Aircraft NOise Prediction Program – Second Generation
bb	Broadband trailing edge self noise
BVI	Blade Vortex Interaction
CAMRAD II	Comprehensive Analytical Model of Rotorcraft Aerodynamics and Dynamics
EPNL	Effective Perceived Noise Level, dB
Lmax	Maximum noise level, A-weighted, dB
loadz	Blade Z direction (vertical) load in airframe axes, + down, N/m. (-loadz) + up
N	Number of blades per rotor
OASPL	Overall Sound Pressure Level, dB
pyaaron	Python tool to aid running AARON
RCOTOOLS	Rotorcraft Optimization Tools
RVLT	NASA Revolutionary Vertical Lift Technology Project
t+l	Thickness and loading (noise)
VTIP	Blade tip speed, ft/sec
"*VTIP/N*"	Refers to specific design concept with tip speed=VTIP and number of blades=N

INTRODUCTION

The NASA Revolutionary Vertical Lift Technology (RVLT) Project has been developing tools to predict rotorcraft attributes for more than a decade (Ref. 1). In aeromechanics and rotorcraft design, these attributes include noise, performance, handling qualities, vibration, and cost. RVLT has also been developing various software packages to link individual, discipline-based prediction tools to create a unified toolchain. As a result, today, the RVLT toolchain covers a broad range of disciplines. In addition to the tools themselves, NASA is seeking to document best practices for using the tools and to provide validation data, such that the toolchain is quantitatively meaningful and may be reliably exercised by conceptual design engineers in the U.S. government, industry, and academia.

Recently, Ref. 2 used the RVLT Toolchain for the practical conceptual design of quieter urban VTOL aircraft. Several concept vehicles were studied in Ref. 2, including a 6-passenger quadrotor, Figs. 1a-1c. This paper addresses source identification and analysis of 6-passenger quadrotor noise, with the goal of providing evidence toward best practices for application of the toolchain.

Figure 1a. NASA 6-passenger quadrotor concept vehicle, shown with 3 blades per rotor, Ref. 2.

The research reported in this paper is a follow-on study to Ref. 2. Here, noise is calculated and analyzed for the quadrotor concept vehicle. The RVLT Toolchain is exercised for this purpose. Noise predictions for three flight conditions (approach, flyover, and takeoff) are obtained for eight tip speeds, ranging from 700 to 375 ft/sec. To maintain blade aspect ratio (with higher solidity), the number of blades is

*Corresponding author. Presented at the VFS Aeromechanics for Advanced Vertical Flight Technical Meeting, San Jose, CA, Jan 25-27, 2022.

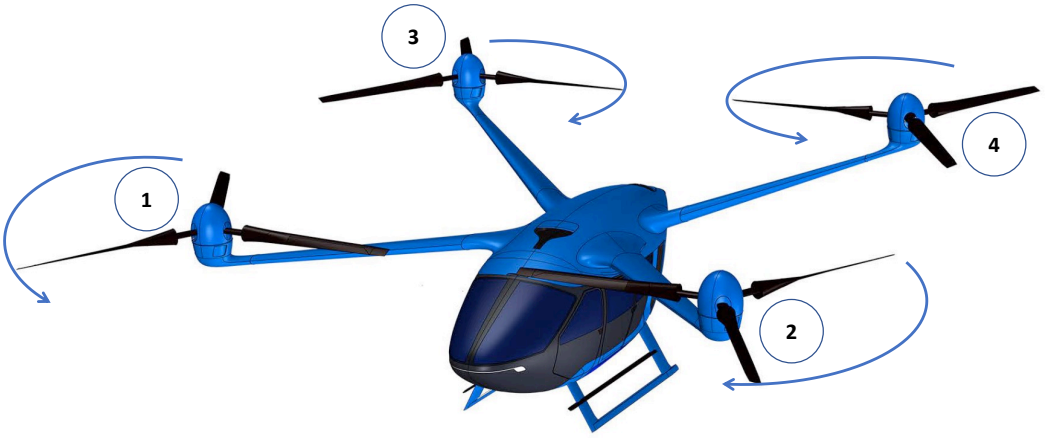

Figure 1b. Quadrotor isometric view, marked with rotor rotation and rotor numbering, Ref. 2.

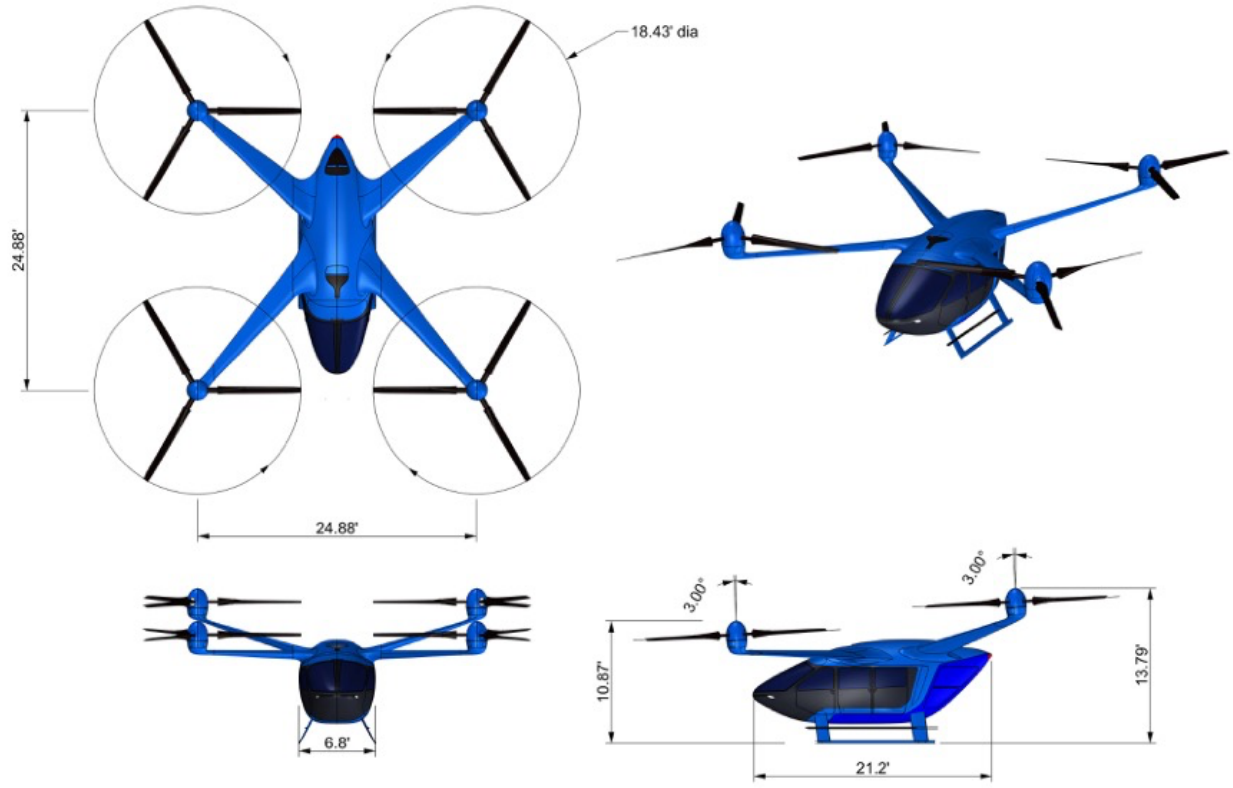

Figure 1c. Quadrotor technical drawings, Ref. 2.

increased from 3 to 7 as tip speed reduces. All vehicles are designed to produce the same thrust (carry 6 passengers, payload=1,200 lb). The study includes analysis of the blade loading to understand noise trends with tip speed and number of blades. Trends of the individual rotor noise sources (thickness, loading, and broadband) are studied. Noise comparison is done using the A-weighted Lmax single sound level, the duration-based effective perceived noise level (EPNL), and the A-weighted Overall Sound Pressure Level (OASPL). The bulk of the results in this paper have been obtained with a rigid blade model. Noise predictions with elastic blades are ongoing, with initial results included in this paper.

This paper includes results for three flight conditions: approach (6-deg descent), level flight flyover, and takeoff. Three design concepts are considered:

1. VTIP=700 ft /sec, 3 blades, denoted as ("700/3")
2. VTIP=550 ft/sec, 3 blades ("550/3")
3. VTIP=375 ft/sec, 7 blades ("375/7")

All three designs are analyzed with rigid blades. One design, "550/3", is also analyzed with elastic blades.

RVLT TOOLCHAIN

Historically, disparate pieces of software, each performing a portion of the VTOL aircraft design and analysis task, have been developed, validated, and employed. These tools have been tailored to subsets of the design problem and developed by domain experts for their own use. As a result, little effort had been expended in ensuring interoperability with other codes, nor with providing ease-of-use for novice or non-expert users.

In place of the loosely organized collection of disparate software, a distinct "toolchain" of VTOL aircraft design and analysis tools is necessary for efficient and successful development of these vehicles. The RVLT project is actively improving the usability and interoperability of the software elements, producing documentation, gathering validation data, and providing test cases, to produce an integrated toolchain.

Figure 2, courtesy of Doug Boyd, NASA Langley, outlines the currently relevant part of the RVLT Toolchain. The rotorcraft comprehensive analysis CAMRAD II (Ref. 3) is used. CAMRAD II provides azimuthal variations of the lifting-line blade loadings (forces) and motions to the acoustic tools. These mostly "dynamics" related quantities are provided by the CAMRAD II "sound sensor." Blade sound sensors provide the information needed to calculate aerodynamically generated sound of the rotor using a compact loading formulation that is consistent with the lifting-line aerodynamic model. Thickness noise is computed using geometry provided by the sound sensor along with user input of the spanwise distribution of blade maximum thickness. There is a sensor for each aerodynamic collocation point (quarter chord, at midpoint of the spanwise aerodynamic panel). All quantities are in airframe axes. A set of Python libraries that serve as application interfaces/wrappers for the execution of CAMRAD II is also a part of the toolchain (RCOTOOLS, Rotorcraft Optimization Tools, Ref. 4). RCOTOOLS is not shown in Fig. 2.

"pyaaron," a Python based wrapper script, provides an interface for application-specific user inputs. pyaaron also extracts sound sensor data that are then passed on to the acoustic tools. The acoustic calculations are done with the following tools: ANOPP2 (Aircraft NOise Prediction Program 2) and AARON (ANOPP2's Aeroacoustic ROtor Noise tool), Ref. 5. In this context, AARON is an ANOPP2 software tool written in Fortran that runs the ANOPP2 Farassat Formulation 1A Function Model (AFFIFM) for tone noise and/or ANOPP2's Self Noise Internal Function Module (ASNIFM) for rotor broadband self noise.

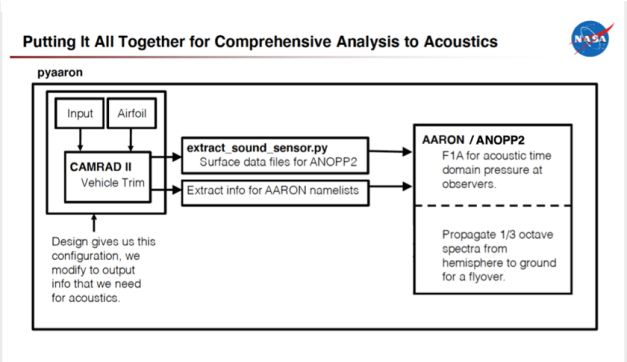

Figure 2. CAMRAD II plus AARON/ANOPP2.

Toolchain Implementation

MacPro/iMac Pro workstations, a MacBook laptop, and the NASA supercomputer Pleaides were used to run the needed, relatively large number of CAMRAD II cases. For the paper results, all acoustic calculations were run serially on the Mac machines.

QUADROTOR MODELING

The CAMRAD II model of the quadrotor is summarized as follows: 4 rotors, collective control, constant RPM, rolled-up free wake (single tip vortex from each rotor blade), and 6-DOF trim (zero forces and moments). The right-front and left-rear rotors turn counterclockwise, and the left-front and right-rear rotors turn clockwise (Fig. 1b). For this study, fully coupled rotor wakes were evaluated. This setting is likely to be the most accurate depiction of the phenomena, as it can capture potentially important interactions due to strong vortices from not only the other blades on the same rotor, but also from another rotor's blades. The quadrotor design has already included a mitigation of rotor-rotor interaction in forward flight by elevating the rear rotors relative to the front rotors. Reference 2 has some discussion on this, and Ref. 6 has the primary discussion of elevating the rear rotors as a design choice. As noted earlier, the concept designs involve 3 to 7 blades per rotor, with the tip speed varying correspondingly from 700 to 375 ft/sec. Detailed design data on the concept vehicles can be found in Ref. 2. Three designs

are considered in the current study: "700/3", "550/3", and "375/7". For these three designs, the quadrotor blade radius is roughly 9 ft (Ref. 2).

Blade Models

Two types of quadrotor blades are considered: rigid and elastic anisotropic blades. The rigid blades have constant (uniform) spanwise properties, and the blade root includes a flap hinge and a pitch bearing. For the elastic blades a fully articulated model is considered – a lag hinge is also included, in addition to the flap hinge and the pitch bearing. Thus, the elastic blade analysis is done for an articulated blade with flap, lag, and torsion degrees of freedom. The elastic anisotropic blades were designed for this paper. The spanwise and cross-sectional properties were obtained using IXGEN/VABS (Refs. 7-8). The elastic blades have nonuniform spanwise blade properties.

A rigid blade analysis was performed for all three designs: "700/3", "550/3", and "375/7". An elastic blade analysis was performed for "550/3" only.

Acoustic Model

The noise tool AARON calculates the 1/3 octave spectrum at each point of a 19x19 hemisphere underneath the vehicle. This calculation is based on the CAMRAD II outputs and other supplemental information and includes both periodic sources (thickness and loading noise) and trailing edge self noise (broadband noise), Ref. 2.

NOISE AND VERTICAL BLADE LOADING

A qualitative analysis of the vertical blade loading (loadz) helps to understand noise trends with tip speed and number of blades. Trends of the individual rotor noise sources (thickness, loading, and broadband) are studied. In this section, the A-weighted Lmax single sound level and the duration-based effective perceived noise level, EPNL, are used to compare noise levels. OASPL predictions are considered in the next section.

The predictions are shown in two ways:

1. Per design (i.e., tip speed/number of blades) for the three flight conditions (approach, flyover, and takeoff).
2. By flight condition, for the three designs.

The predictions are shown in three types of plots: 1) blade loading as contour plots for the front right rotor, 2) blade loading as azimuthal variations at 0.75R for the front right rotor, and 3) quadrotor noise sources (all four rotors). To reiterate, blade loadings are studied only for rotor #1 (front right rotor, counterclockwise rotation, Figs. 1b-1c), while the noise results include contributions from all four rotors. Figures 3-5 show the results per design. Figures 6-8 show the results by flight condition. In Figs. 3-8, the negative of the vertical blade loading loadz is shown. Note that -loadz is + up.

Broadly, Figs. 3-8 show that for all three flight conditions, "700/3" has the highest noise level and "375/7" the lowest, with "550/3" falling in between. Also, approach is the loudest condition and takeoff the quietest with flyover falling in between, though the flyover "375/7" noise level is almost as high as the other designs.

Based on a visual study of the 0.75R azimuthal variations and the contour plots (Figs. 3-8), Tables 1a-1b show the basic characteristics of the BVI events, which substantially affect the loading noise. Tables 1a-1b characterize BVIs by 1) the number of occurrences, and 2) qualitatively, their strength, respectively.

Table 1a. Number of BVIs, per design and flight condition (based on 0.75R azimuthal variation, ~0 denotes very weak BVI) – front right rotor.

	Approach		Flyover		Takeoff	
Design	Adv.	Ret.	Adv.	Ret.	Adv.	Ret.
700/3	7	3	4	~ 0	0	0
550/3	5	2	3	0	0	0
375/7	~ 0	~ 0	4	1	0	0

Adv.: advancing side. Ret.: retreating side

Table 1b. Strength of BVIs, per design and flight condition (based on 0.75R azimuthal variations) – front right rotor.

	Approach		Flyover		Takeoff	
Design	Adv.	Ret.	Adv.	Ret.	Adv.	Ret.
700/3	Strong	Strong	Strong	None	None	None
550/3	Mild	Mild	Mild	None	None	None
375/7	None	None	Weak	Weak	None	None

Adv.: advancing side. Ret.: retreating side

In Table 1a, the number of BVIs were determined by counting the peaks in the loadz 0.75R azimuthal variation (for example, Fig. 3d) and also by a visual study of the hot spots in the contour plots (for example, Figs. 3a-3c). In Table 1b, BVI strength was estimated by eyeballing the loadz derivative.

Note: In this initial study, only the blade loading for the front right rotor is considered. Future studies may consider the blade loading for all four rotors. The rear rotors will likely see a lot of BVIs in descent and probably during takeoff.

Noise, Per Design

"700/3": Figure 3 shows that approach noise is the highest and takeoff noise the lowest, with flyover noise falling in between. Figure 3 and Tables 1a-1b show that during approach (6-deg descent) there are multiple, strong BVIs on the advancing and retreating sides, resulting in relatively high loading noise and EPNL. In flyover, BVI effects are still present on the advancing side but there seem to be no BVI events on the retreating side, resulting in lower loading noise and EPNL. During takeoff there are no BVIs, resulting in the lowest loading noise and EPNL. During takeoff the wake is blown back ("quickly convecting wake," Ref. 2, p. 12, 2nd para). For

all three flight conditions, compared to the loading noise, the thickness noise is smaller, and does not significantly affect the total noise. Broadband noise is roughly the same for all three flight conditions.

"550/3": Figure 4 and Tables 1a-1b show that loading and noise results for "550/3" are similar to "700/3", though the BVI events are fewer and milder, implying "550/3" is a quieter design. Reducing the tip speed from 700 to 550 ft/sec while retaining the 3-bladed configuration reduces noise.

"375/7": Figure 5 and Tables 1a-1b show that, compared to "700/3" and "550/3", the "375/7" approach loading noise has been reduced – no significant BVI events on either the advancing or retreating side. "375/7" is the quietest design during approach and takeoff, but in flyover has roughly the same noise level as the 3-bladed designs. Takeoff noise is the lowest due to reduced loading noise (and lower broadband noise). In Fig. 5e, the thickness noise is negative for all three flight conditions. This is a result of A-weighting, with the unweighted thickness noise being positive for all three flight conditions (unweighted results are not included in this paper).

Noise, By Flight Condition

Approach: Figure 6 shows that the loadz harmonic content and azimuthal variations for the 3-bladed "700/3" and "550/3" designs are roughly similar. There is some attenuation of the harmonics at 550 ft/sec, and much more so for the 7-bladed 375 ft/sec design. Figure 6 and Tables 1a-1b show that the "700/3" and "550/3" designs have multiple BVI events (advancing and retreating sides). The "375/7" design has no significant BVIs, and much smaller higher-harmonic content, resulting in the lowest loading noise and EPNL. Broadband noise is roughly the same for all three designs.

Flyover: Figure 7 and Tables 1a-1b show that compared to approach (Fig. 6, Tables 1a-1b), BVI effects in flyover seem less, except for "375/7" in which there are some advancing side BVI effects and a smaller BVI effect on the retreating side. The "700/3" and "550/3" flyover noise levels are smaller than during approach. "375/7" has higher loading noise and EPNL in flyover compared to approach. The noise results in Fig. 7 show that for flyover, the benefit of reducing the tip speed does not seem to be significant. As in approach, the broadband noise stays roughly the same for all three designs.

Takeoff: Figure 8 and Tables 1a-1b show that takeoff is characterized by an absence of BVI effects. Compared to approach and flyover (Figs. 6-7, Tables 1a-1b), there does not seem to be any significant BVI during takeoff (Fig. 8) for the front right rotor– the wake is blown back and down at takeoff but could cause BVI for the rear rotors. The quadrotor noise results in Fig. 8 show that reducing the tip speed results in diminished benefits at takeoff. Unlike the approach and flyover conditions where the broadband noise stayed roughly the same at all three tip speeds, in the takeoff condition lower tip speeds reduce the broadband noise. Takeoff noise levels are smaller than the approach and flyover noise levels – takeoff is the quietest condition based on the current results.

OASPL – PEAK VALUES AND TIME-HISTORIES

The A-weighted OASPL results presented in this section are, as expected, consistent with the A-weighted Lmax results that were presented and discussed in the previous section. To avoid repetition, only salient observations are presented here.

Peak A-weighted OASPL

Table 2 shows the peak A-weighted OASPL noise for the three designs and the three flight conditions. Total, broadband (self), and thickness and loading noise contributions are shown in Table 2. The following observations, based on Table 2, are consistent with the results of the previous section:

1. Broadband (self) noise during approach and flyover is roughly the same for all three designs. Takeoff broadband noise is much lower, especially for the "375/7" design (the reason for this requires further study).
2. During approach and flyover, the thickness and loading (t+l) noise is the main component except for "375/7" in approach (where very little BVI effects are seen for the front right rotor).
3. Takeoff is quietest for all designs. The t+l noise is low because of the wake being blown back.

Table 2. Peak A-weighted OASPL, per design and flight condition, dBA.
Noise source legend: total/**broadband**/**thickness+loading**

Design	Approach	Flyover	Takeoff
700/3	82/**62**/**82**	74/**60**/**74**	57/**56**/**54**
550/3	72/**61**/**72**	72/**58**/**72**	56/**54**/**51**
375/7	62/**60**/**58**	71/**59**/**71**	49/**48**/**41**

OASPL Time-Histories

OASPL time-histories are shown in Figs. 9-16. Figure 9 summarizes the total noise for all nine cases (three designs, three flight conditions). The "700/3" approach peak is the largest and the "375/7" takeoff peak the smallest. The rest of the time-histories, Figs. 10-16, are listed below, along with brief descriptions:

a. Figure 10: Total noise per design, three flight conditions.
b. Figure 11: Broadband (bb) and thickness and loading (t+l) contributions per design, three flight conditions.
c. Figure 12: Total noise by flight condition, three designs.
d. Figure 13: Broadband and thickness and loading contributions by flight condition, three designs
e. Figure 14: Approach noise (total, broadband, and thickness and loading), three designs.

f. Figure 15: Flyover noise (total, broadband, and thickness and loading), three designs.
g. Figure 16: Takeoff noise (total, broadband, and thickness and loading), three designs.

Figures 10-16 provide the time-histories on which Table 2 is based. The data in Table 2 are consistent with their corresponding values presented in the previous section. To summarize:

a. In the approach time-histories (Figs. 12a), the total noise increases rapidly, and the post-peak decrease is much slower. This is due to the t+l noise contribution (Fig. 14). This behavior is most evident for "700/3".
b. For "375/7", the broadband time-history (Fig. 11c) shows that the takeoff peak occurs earlier compared to the approach and flyover peaks and is less sharp.

The underlying reasons for the above trends require further study.

NOISE, WITH ELASTIC BLADES

All results presented so far were obtained for quadrotors with rigid uniform blades, with each blade root having a flap hinge and a pitch bearing. To date, limited results with elastic anisotropic nonuniform blades on the quadrotor conceptual vehicle have been obtained and are now presented in this section. A fully articulated blade with flap and lag hinges and a pitch bearing is considered. In this section, the "550/3" (VTIP=550 ft/sec, 3 blades) design concept is considered for further study. Initial results for the approach flight condition are presented here. To ensure that the effect of blade elasticity on quadrotor noise is studied in a consistent manner, the following four analytical blade models must be considered, and the corresponding noise results compared. In increasing complexity, the blade models are:

1. Rigid blade with uniform spanwise properties, with flap hinge and pitch bearing (all noise results shown in the preceding sections are based on this blade model).
2. Rigid blade with uniform spanwise properties, with flap and lag hinges and pitch bearing.
3. Rigid blade with nonuniform spanwise properties, with flap and lag hinges and pitch bearing. This is a rigid beam version of the elastic blade in item 4.
4. Elastic anisotropic blade with nonuniform spanwise and cross-sectional properties, with flap and lag hinges and pitch bearing.

Results associated with blade models 2-4 are summarized here and compared with the relevant results using blade model 1 presented in previous sections. Detailed analysis of the elastic blade loading (contours and time-histories) and associated quadrotor OASPL time-histories is ongoing. Only the quadrotor A-weighted Lmax and EPNL noise levels are included here.

Elastic Nonuniform Blade Frequencies

Table 3 shows "first pass" natural frequencies for the "550/3" (VTIP=550 ft/sec, 3 blades) design concept.

Table 3. Blade frequencies, design concept "550/3" (VTIP=550 ft/sec, 3 blades).

Mode	Frequency, per/rev
1st lag	0.27
1st flap	1.03
2nd flap	2.91
Torsion	6.41
2nd lag	7.69
3rd flap	11.38

Noise Comparisons

Table 4 shows predicted A-weighted Lmax and EPNL corresponding to the four blade models (approach, 6 deg descent). Figure 17 shows the same information as a column chart. Based on this initial limited study, the following observations can be made:

a) For all four blade models, only the loading noise is different – the thickness and broadband noise are roughly the same for all four models. Thus, the total noise trend is the same as the loading noise trend.
b) The addition of the lag hinge to the rigid blade with uniform properties reduces the loading noise by ~1.5 dB (blade models 1 and 2, Table 4 last row).
c) For the current rigid nonuniform blade, a further ~1 dB reduction in loading noise is obtained (compared to the rigid uniform blade, blade models 2 and 3).
d) Results for the rigid nonuniform and elastic blades do not show any significant difference in the noise levels (blade models 3 and 4). The blade radius is ~9 ft and the design RPM is ~584 for the "550/3" design. For this relatively short blade (compared to a regular helicopter that may have a radius two to three times 9 ft), elastic effects on the noise may not be significant. This result needs to be confirmed through further analysis with current and other blade designs.
e) Even though the total (and loading) A-weighted Lmax noise levels show sensitivity to the current blade models, EPNL is roughly the same for all blade models.

CONCLUSIONS

The NASA Revolutionary Vertical Lift Technology (RVLT) Project conceptual design toolchain was exercised to predict the acoustics of the NASA 6-passenger quadrotor concept vehicle. The study included qualitative analysis of the blade vertical loading to understand noise trends with tip speed and number of blades. Trends of the individual rotor noise sources (thickness, loading, and broadband) were studied. Noise comparison was done using the A-weighted Lmax single sound level, the duration-based effective perceived noise

level (EPNL), and the A-weighted Overall Sound Pressure Level (OASPL).

Quadrotor noise from all four rotors was predicted and analyzed for three flight conditions: approach (6-deg descent), level flight flyover, and takeoff. Three concept vehicles were considered:

1. Tip speed=700 ft/sec, 3 blades ("700/3")
2. Tip speed=550 ft/sec, 3 blares ("550/3")
3. Tip speed=375 ft/sec, 7 blades ("375/7")

The bulk of the results in this paper were obtained with a rigid uniform blade model, with a flap hinge and a pitch bearing. Noise predictions with elastic blades have been initiated and are ongoing, with initial results included in this paper for the "550/3" design.

The results were presented in two ways: 1) per design, three flight conditions, and 2) by flight condition, three designs. Also, the predictions were shown in three types of plots: 1) blade loading as contour plots, 2) blade loading as azimuthal variations at 0.75R, and 3) quadrotor noise sources.

The qualitative study was based on the vertical blade loading for the front right rotor. However, the noise calculations included all four rotors. Specific conclusions are as follows:

1. Broadly, for all three flight conditions, "700/3" had the highest EPNL and "375/7" the lowest, with "550/3" falling in between. Also, approach had the highest EPNL and takeoff the lowest, with flyover falling in between. In contrast, the flyover "375/7" noise level was almost as high as the flyover levels of the other designs.

2. A qualitative study of the vertical blade loading for the front right rotor showed that:
    a. During approach multiple, strong BVIs occurred on the advancing and retreating sides for "700/3" and "550/3", but for "375/7" only weak BVIs were present. Consistent with this BVI scenario, "700/3" had the highest loading noise (and EPNL) and "375/7" the lowest loading noise (and EPNL), with "550/3" falling in between.
    b. All three designs encountered a few BVIs on the advancing side during flyover with their effects being strongest in the "700/3" design and weakest in the "375/7" design. One weak BVI was identified on the retreating side in the "375/7" design. This mix of BVI events resulted in comparable loading noise levels and EPNL for all three designs.
    c. For all three designs, the takeoff condition was characterized by a lack of BVIs for the front right rotor due to the rotor wake being blown back, resulting in the lowest loading noise and EPNL.

3. The OASPL peak values and time-history results showed trends consistent with the above conclusions. Also,
    a. Broadband (self) noise during approach and flyover was roughly the same for all three designs. Takeoff broadband noise was much lower, especially for "375/7".
    b. During approach and flyover, the thickness and loading (t+l) noise was the main component except for "375/7" in approach (where very little BVI effects were seen).

4. For "550/3", initial, limited results were obtained with three additional blade models. The effect of the addition of a lag hinge, nonuniform blade properties, and blade elasticity were studied systematically. Specific findings include:
    a. The addition of a lag hinge to the rigid unform blade resulted in a drop in the quadrotor loading noise of about 1.5 dB.
    b. Nonuniformity in rigid blade properties resulted in an additional drop in the loading noise of about 1 dB.
    c. Quadrotor noise was not significantly affected by blade elasticity. This result needs to be verified through further analysis with current and other blade designs.

Author contact:
Sesi Kottapalli sesi.b.kottapalli@nasa.gov
Christopher Silva christopher.silva@nasa.gov

ACKNOWLEDGMENTS

Helpful discussions with the following colleagues are gratefully acknowledged: Wayne Johnson, Larry Meyn, and Bill Warmbrodt. Special thanks to Doug Boyd (NASA Langley) for going above and beyond the call of duty to get the first author's acoustic simulations up and running.

REFERENCES

1. Yamauchi, G., "A Summary of NASA Rotary Wing Research: Circa 2008–2018," NASA/TP 2019-220459, December 2019.
2. Silva, C. and Johnson, W., "Practical Conceptual Design of Quieter Urban VTOL Aircraft," The Vertical Flight Society 77th Annual Forum Proceedings, Virtual, May 2021.
3. Johnson, W., "CAMRAD II, Comprehensive Analytical Model of Rotorcraft Aerodynamics and Dynamics," Johnson Aeronautics, Palo Alto, CA, 1992-1999.
4. Meyn, L., "Rotorcraft Optimization Tools: Incorporating Rotorcraft Design Codes into Multi-Disciplinary Design, Analysis, and Optimization," AHS Technical Meeting on Aeromechanics Design for Vertical Lift, San Francisco, CA, January 2018.

5. Lopes, L., Burley, C., “Design of the Next Generation Aircraft Noise Prediction Program: ANOPP2,” AIAA 2011-2854 17th AIAA/CEAS Aeroacoustics Conference, Portland, OR, June 2011.
6. Johnson, W, Silva, C, and Solis, E, “Concept Vehicles for VTOL Air Taxi Operations,” AHS Technical Conference on Aeromechanics Design for Transformative Vertical Flight, San Francisco, CA, January 16-19, 2018.
7. Rohl, P.J., Dorman, P., Cesnik, C.E.S. and Kumar, D., “IXGEN—A Modeling Tool for the Preliminary Design of Composite Rotor Blades.” American Helicopter Society Future Vertical Lift Aircraft Design Conference, San Francisco, CA, January 2012.
8. Palacios, R. and Cesnik, C. E. S., “Geometrically Nonlinear Theory of Composite Beams with Deformable Cross Sections,” *AIAA Journal*, Vol. 46, No. 2, February 2008

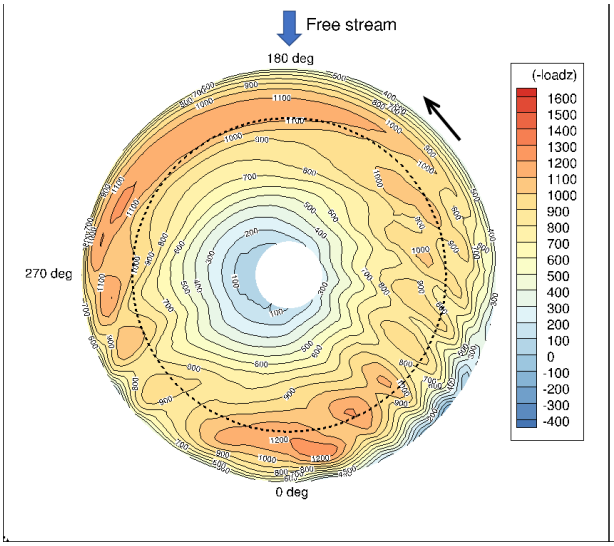

Figure 3a. Approach, 700 ft/sec, 3 blades.

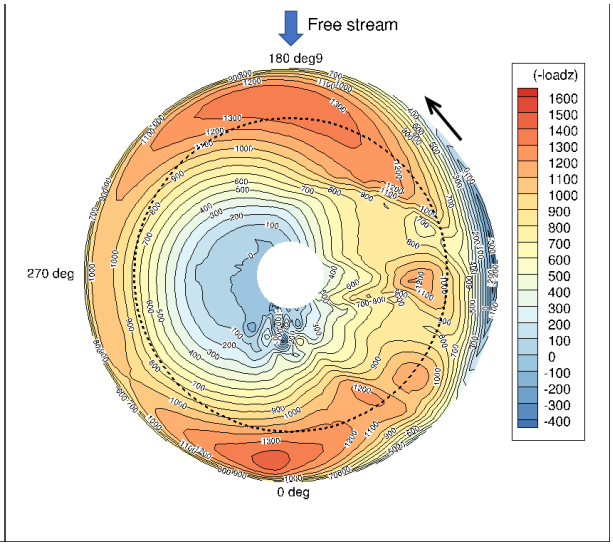

Figure 3b. Flyover, 700 ft/sec, 3 blades.

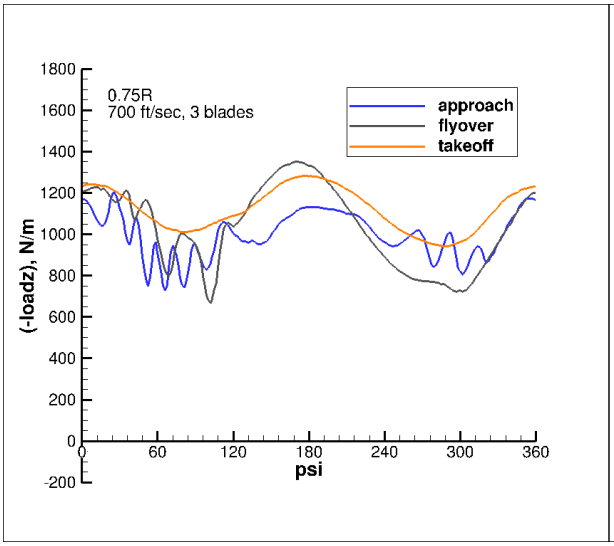

Figure 3d. 0.75R, 3 conditions, 700 ft/sec, 3 blades.

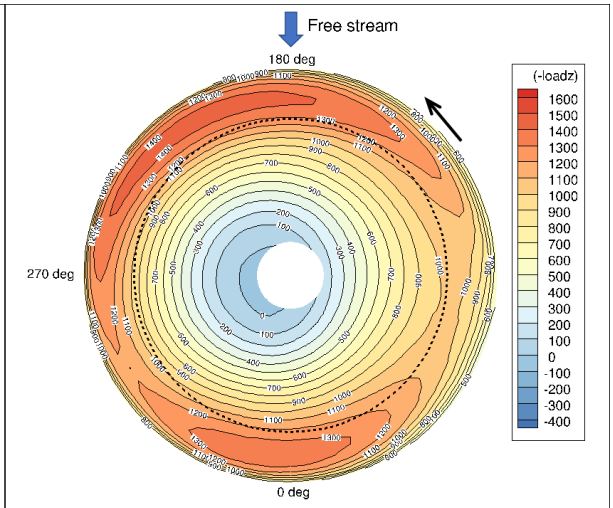

Figure 3c. Takeoff, 700 ft/sec, 3 blades.

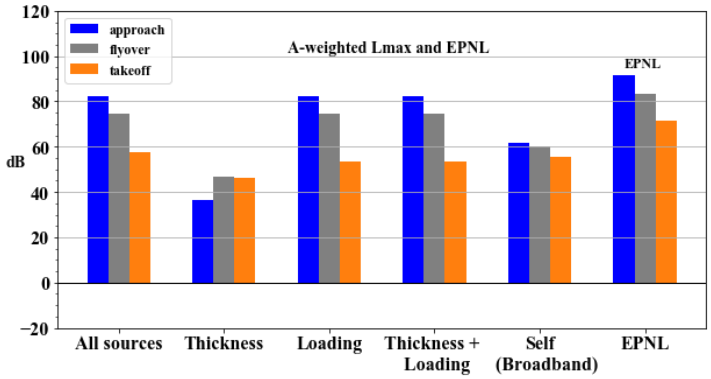

Figure 3e. Quadrotor noise sources (all four rotors), 3 conditions, 700 ft/sec, 3 blades.

Figures 3a-3e. Vertical blade loading and quadrotor noise sources for VTIP=700 ft/sec, 3 blades (3 flight conditions). Dashed circle (3a-3c) represents 0.75R. (-loadz) + up, N/m.

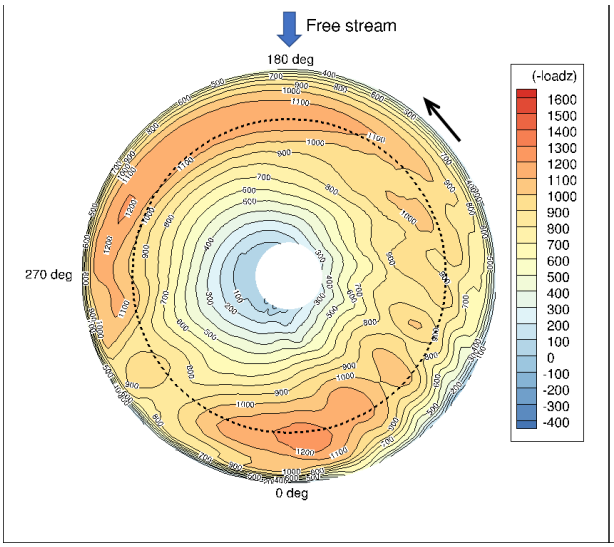

Figure 4a. Approach, 550 ft/sec, 3 blades.

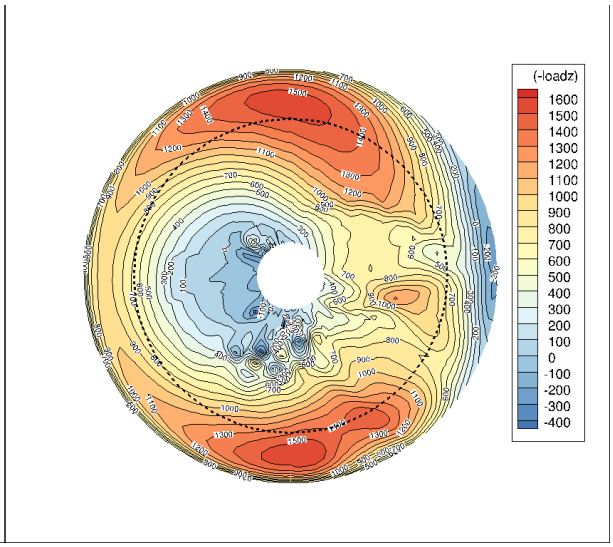

Figure 4b. Flyover, 550 ft/sec, 3 blades.

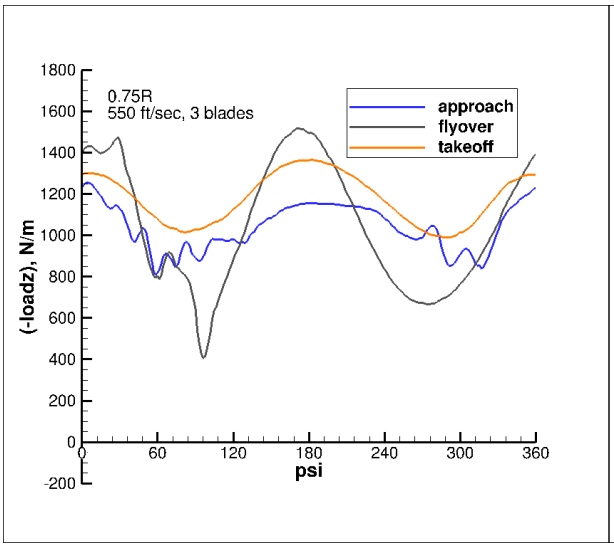

Figure 4d. 0.75R, 3 conditions, 550 ft/sec, 3 blades.

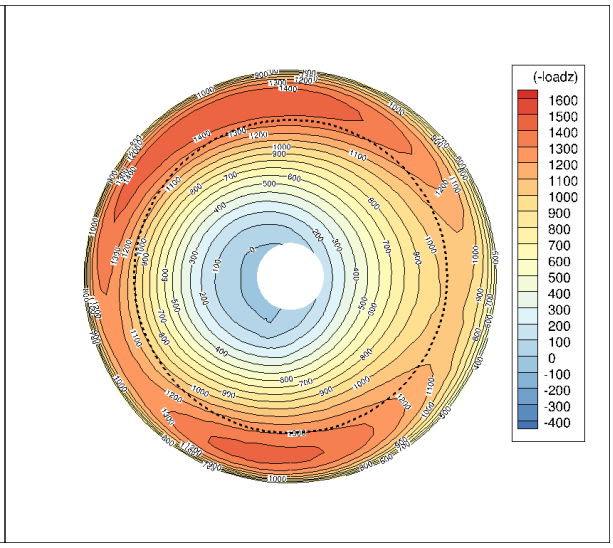

Figure 4c. Takeoff, 550 ft/sec, 3 blades.

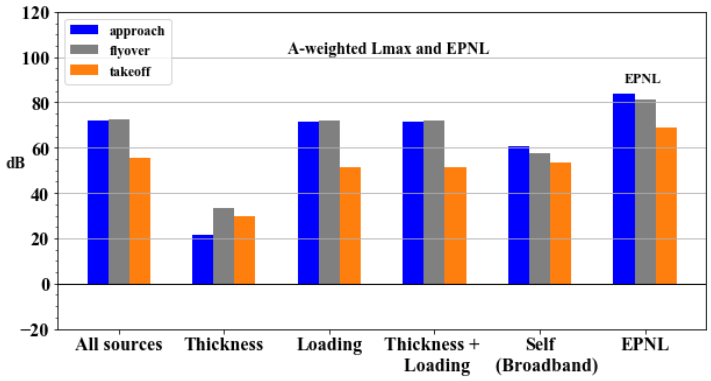

Figure 4e. Quadrotor noise sources (all four rotors), 3 conditions, 550 ft/sec, 3 blades.

Figures 4a-4e. Vertical blade loading and quadrotor noise sources for VTIP=550 ft/sec, 3 blades (3 flight conditions). Dashed circle (4a-4c) represents 0.75R. (-loadz) + up, N/m.

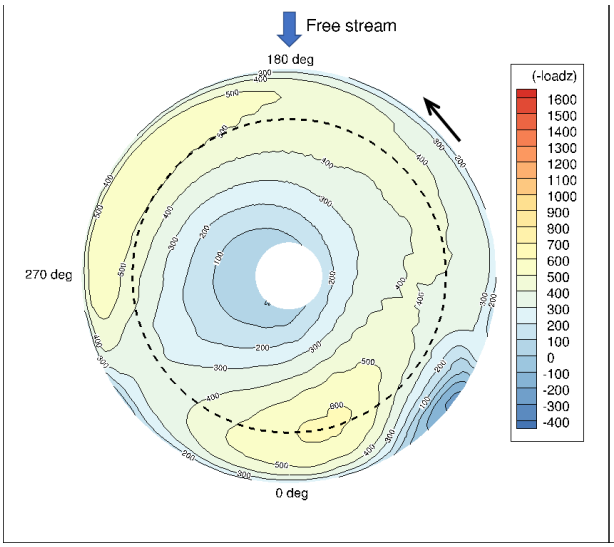

Figure 5a. Approach, 375 ft/sec, 7 blades.

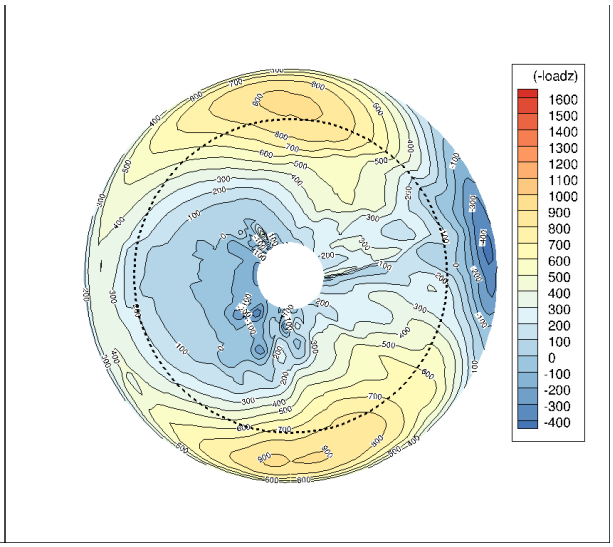

Figure 5b. Flyover, 375 ft/sec, 7 blades.

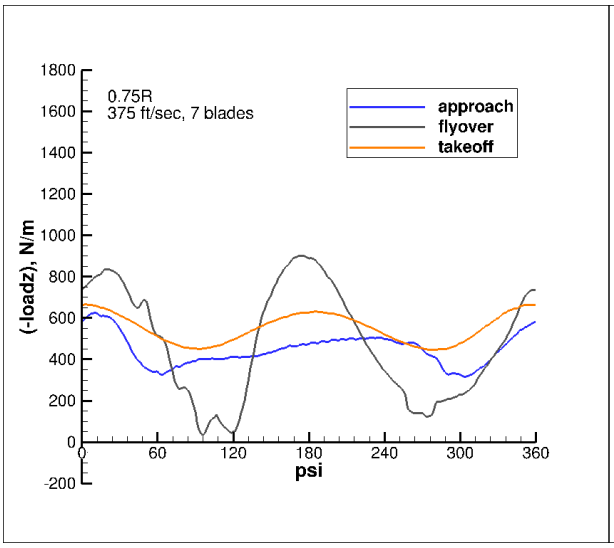

Figure 5d. 0.75R, 3 conditions, 375 ft/sec, 7 blades.

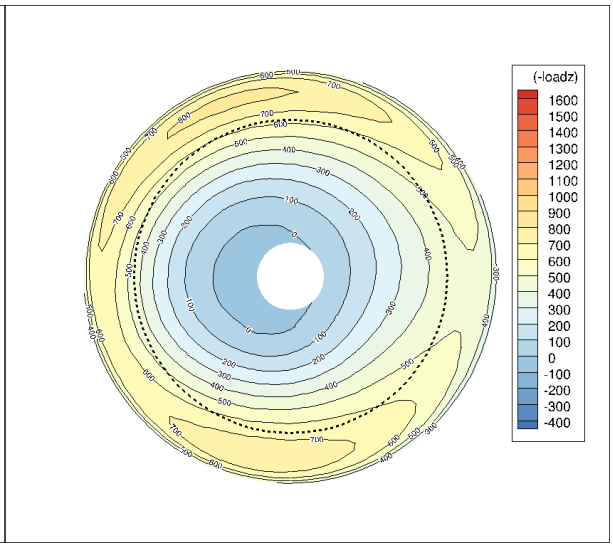

Figure 5c. Takeoff, 375 ft/sec, 7 blades.

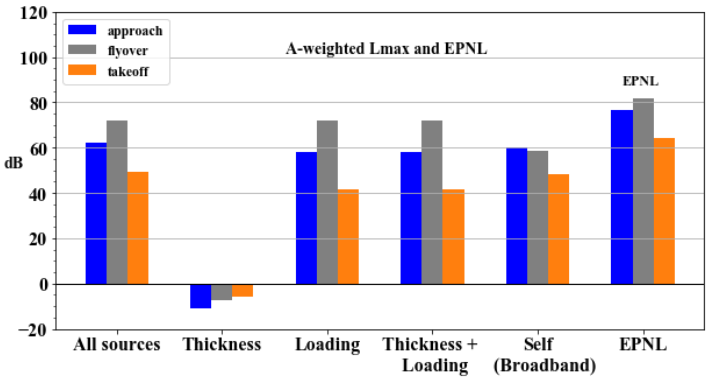

Figure 5e. Quadrotor noise sources (all four rotors), 3 conditions, 375 ft/sec, 7 blades.

Figures 5a-5e. Vertical blade loading and quadrotor noise sources for VTIP=375 ft/sec, 7 blades (3 flight conditions). Dashed circle (5a-5c) represents 0.75R. (-loadz) + up, N/m.

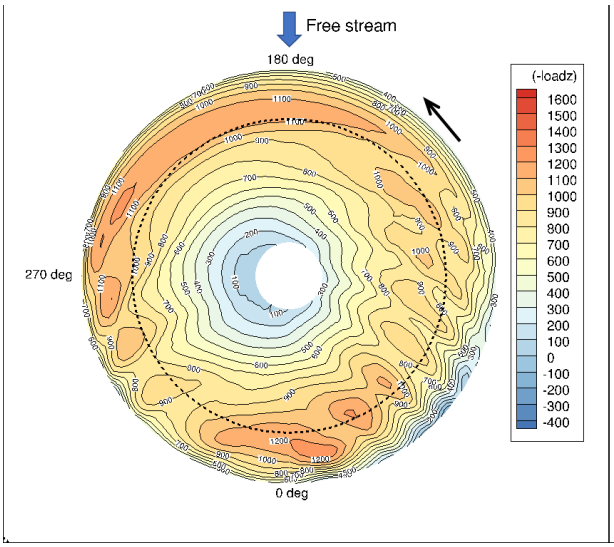

Figure 6a. Approach, 700 ft/sec, 3 blades.

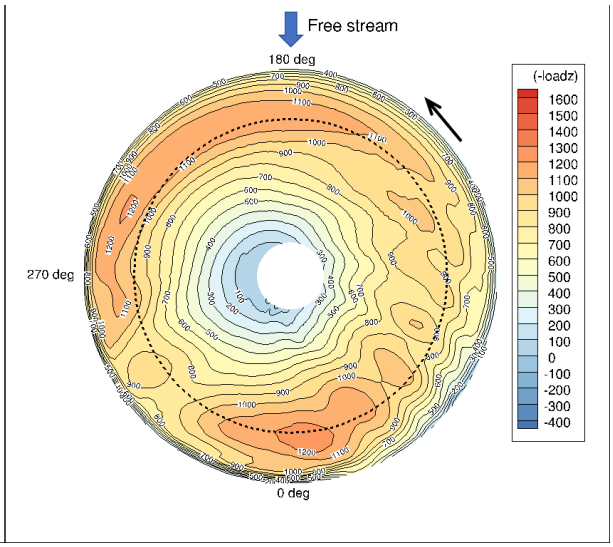

Figure 6b. Approach, 550 ft/sec, 3 blades.

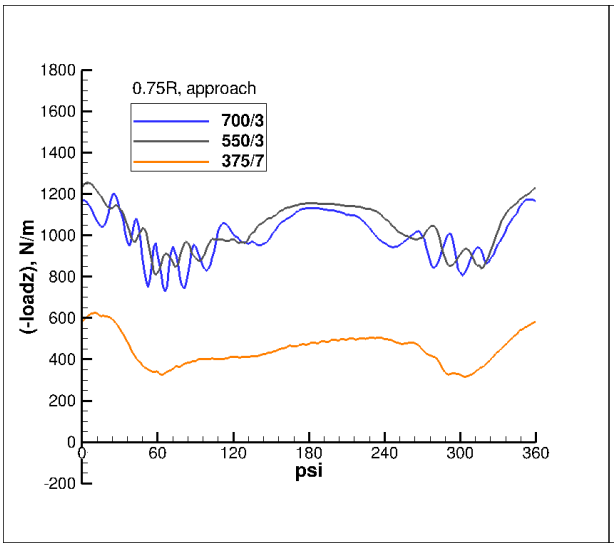

Figure 6d. 0.75R, approach, 3 designs.

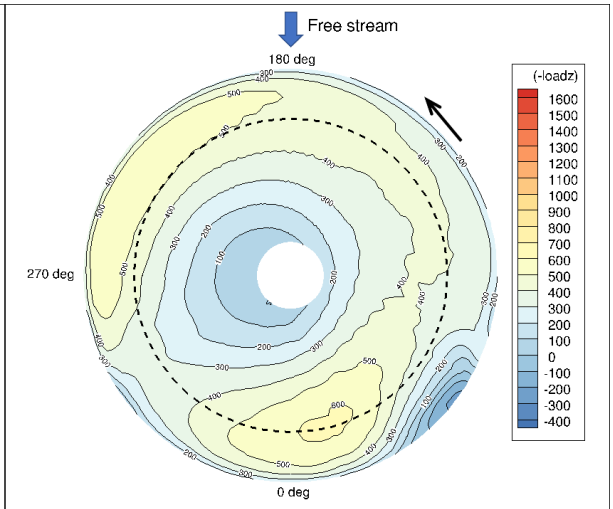

Figure 6c. Approach, 375 ft/sec, 7 blades.

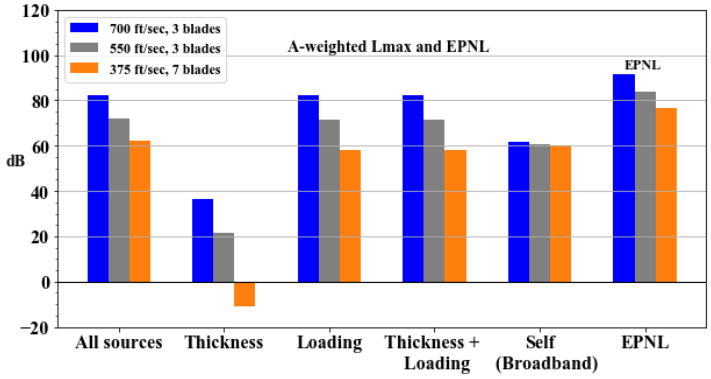

Figure 6e. Quadrotor noise sources (all four rotors), approach, 3 designs.

Figures 6a-6e. Approach vertical blade loading and quadrotor noise sources, 3 designs (tip speed/# of blades). Dashed circle (6a-6c) represents 0.75R. (-loadz) + up, N/m.

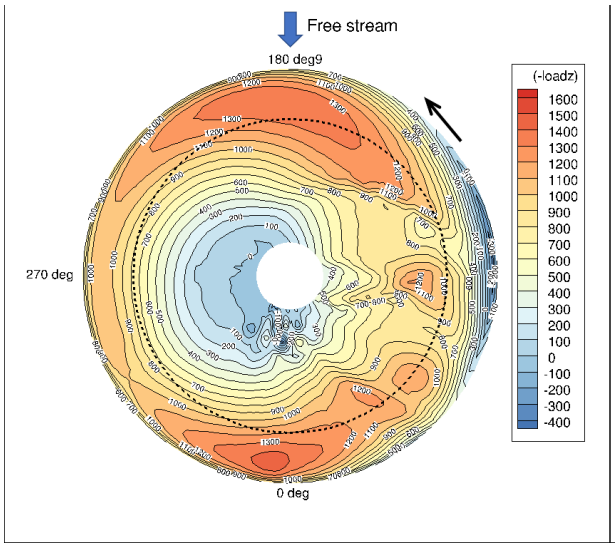

Figure 7a. Flyover, 700 ft/sec, 3 blades.

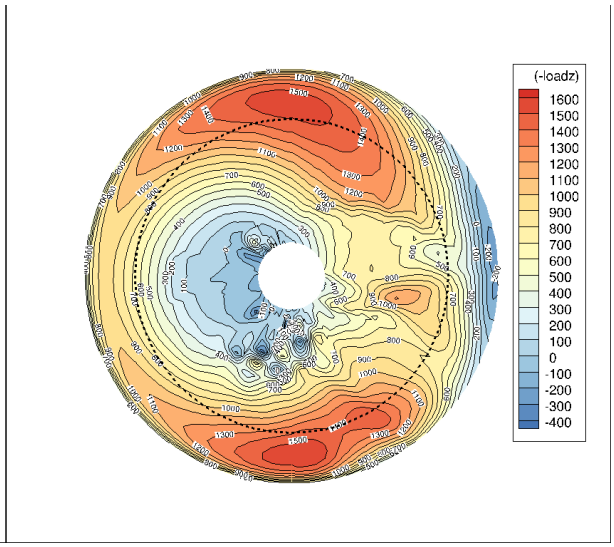

Figure 7b. Flyover, 550 ft/sec, 3 blades.

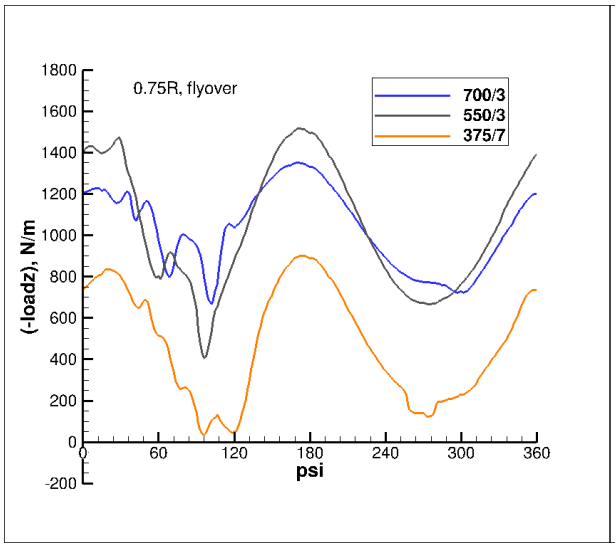

Figure 7d. 0.75R, flyover, 3 designs.

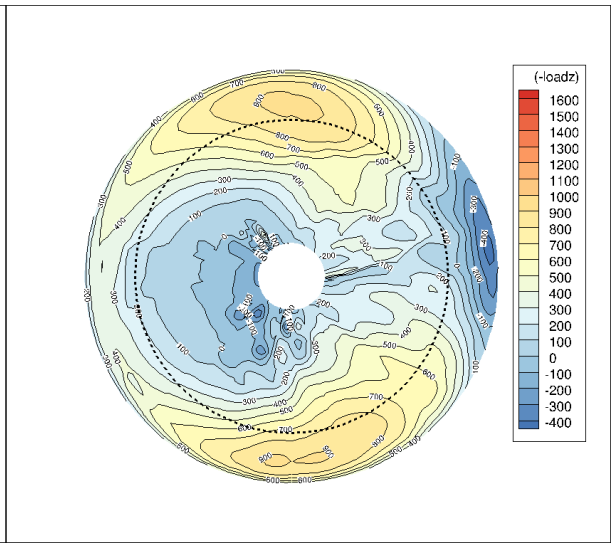

Figure 7c. Flyover, 375 ft/sec, 7 blades.

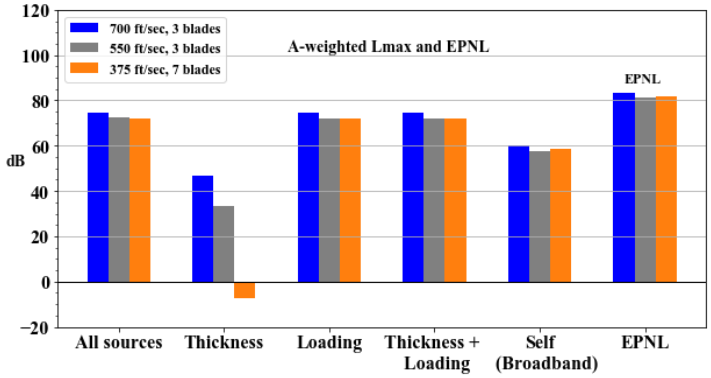

Figure 7e. Quadrotor noise sources (all four rotors), flyover, 3 designs.

Figures 7a-7e. Flyover vertical blade loading and quadrotor noise sources, 3 designs (tip speed/# of blades). Dashed circle (7a-7c) represents 0.75R. (-loadz) + up, N/m.

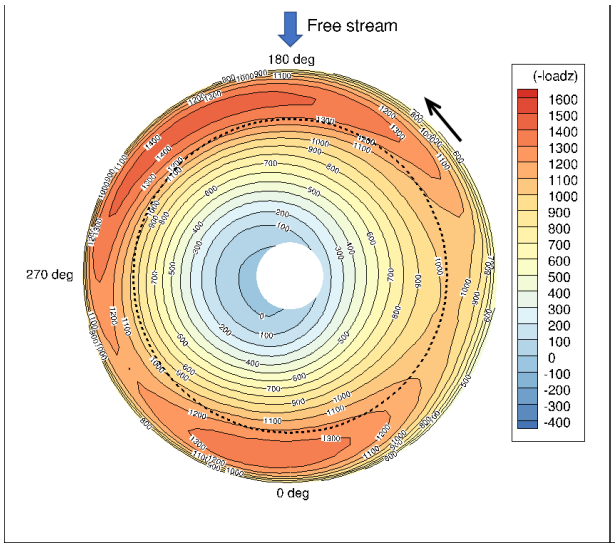

Figure 8a. Takeoff, 700 ft/sec, 3 blades.

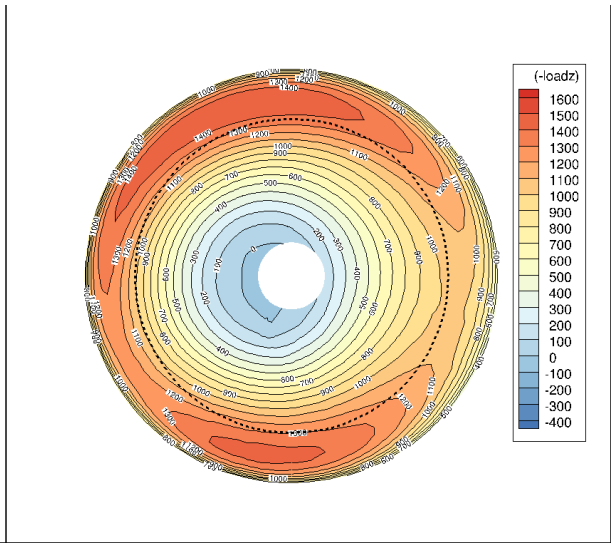

Figure 8b. Takeoff, 550 ft/sec, 3 blades.

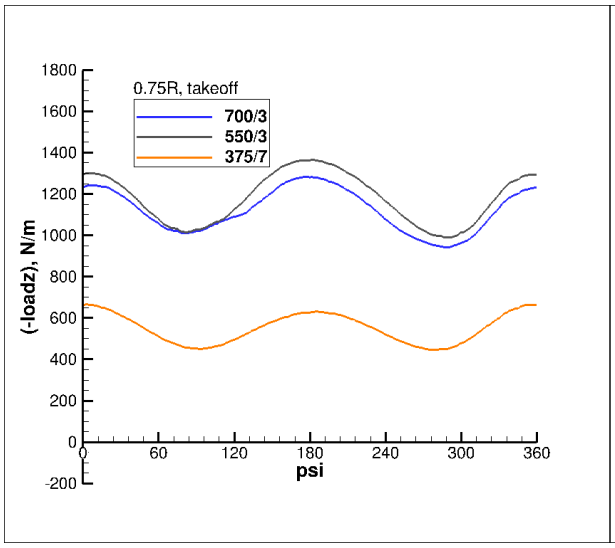

Figure 8d. 0.75R, takeoff, 3 designs.

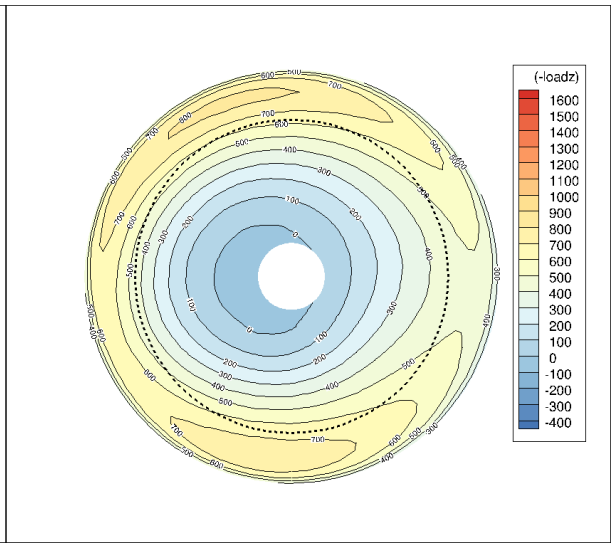

Figure 8c. Takeoff, 375 ft/sec, 7 blades.

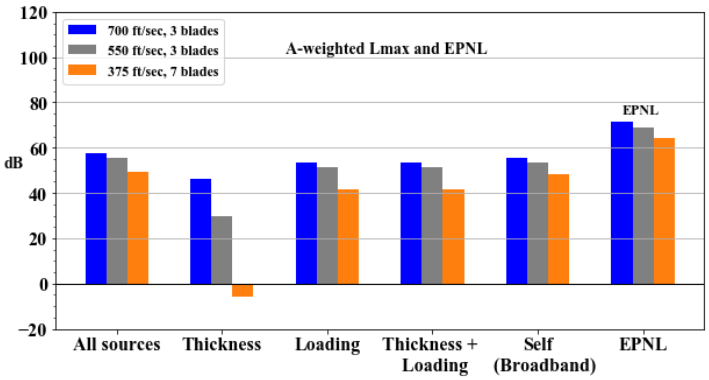

Figure 8e. Quadrotor noise sources (all four rotors), takeoff, 3 designs.

Figures 8a-8e. Takeoff vertical blade loading and quadrotor noise sources, 3 designs (tip speed/# of blades). Dashed circle (8a-8c) represents 0.75R. (-loadz) + up, N/m.

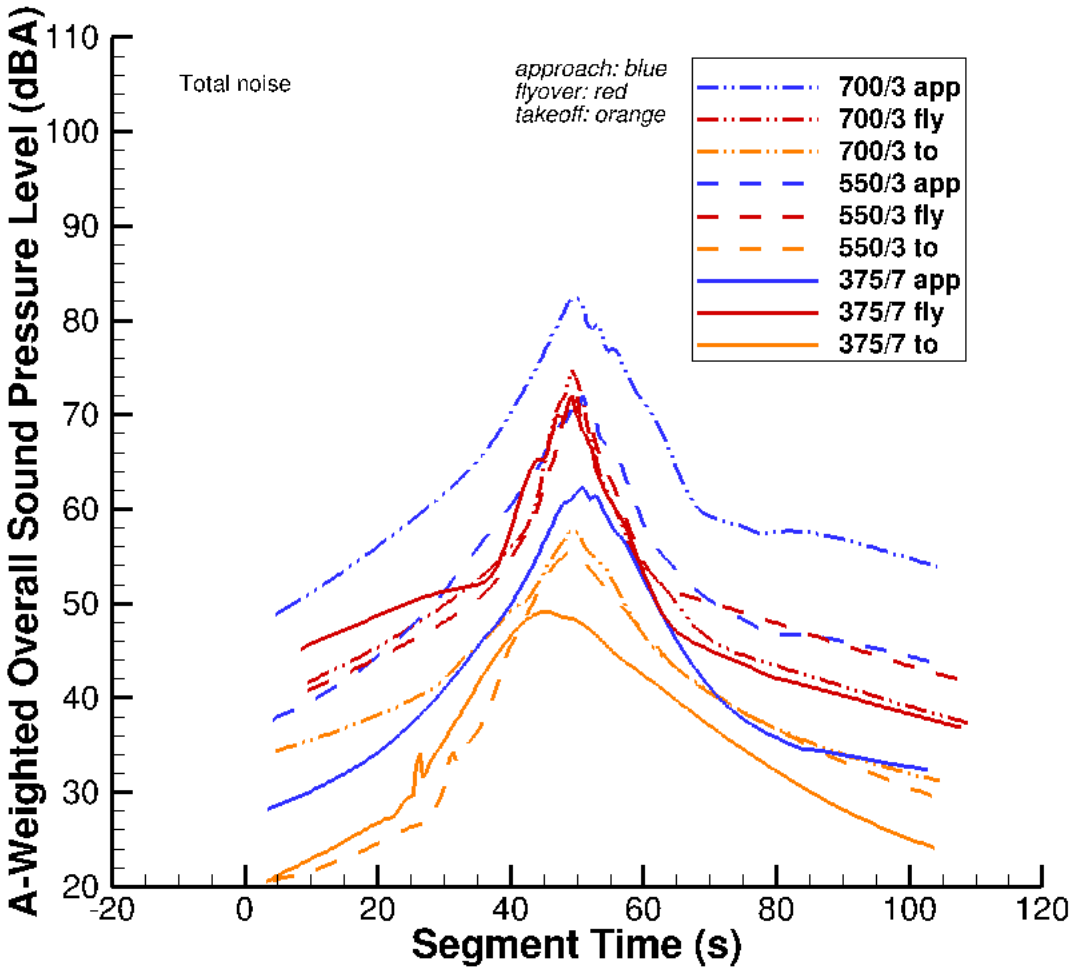

Figure 9. Total A-weighted OASPL noise, three designs, three flight conditions. "700/3" denotes VTIP=700 ft/sec and 3 blades, for example.

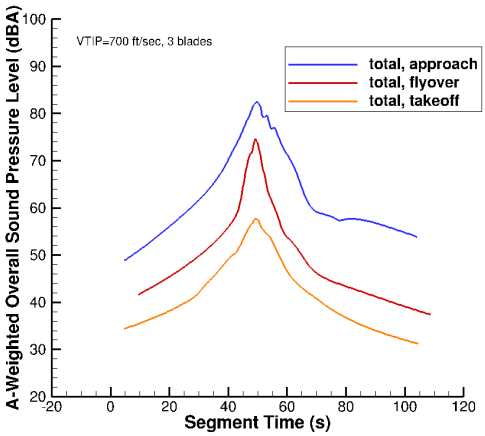

Figure 10a. VTIP=700 ft/sec, 3 blades, 3 flight conditions.

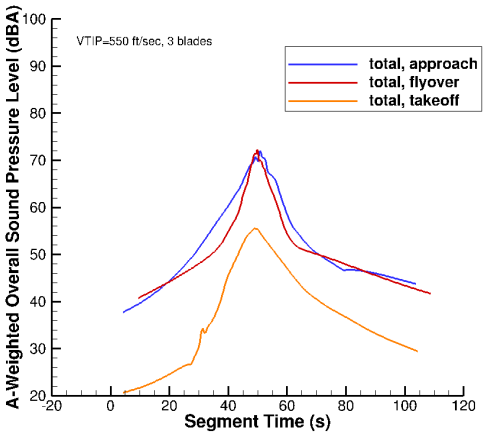

Figure 10b. VTIP=550 ft/sec, 3 blades, 3 flight conditions.

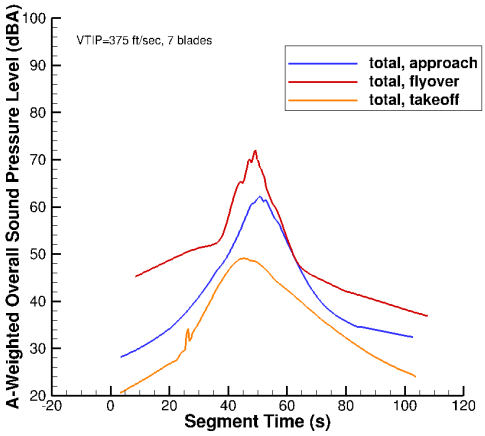

Figure 10c. VTIP=375 ft/sec, 7 blades, 3 flight conditions.

Figures 10a-10c. Total noise per design (i.e., tip speed/number of blades), 3 flight conditions.

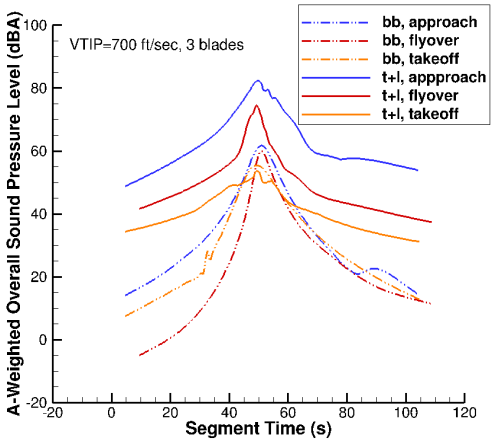

Figure 11a. VTIP=700 ft/sec, 3 blades, 3 flight conditions.

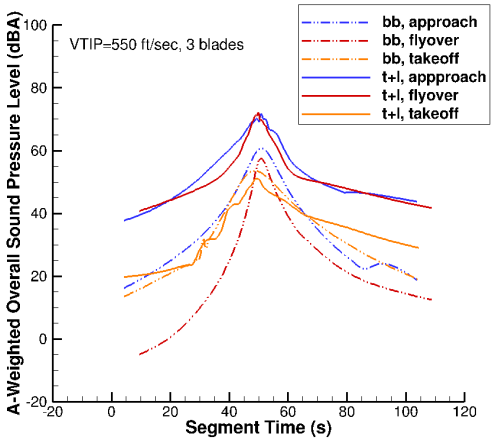

Figure 11b. VTIP=550 ft/sec, 3 blades, 3 flight conditions.

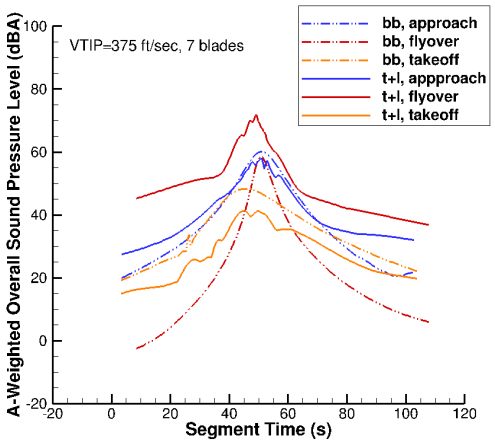

Figure 11c. VTIP=375 ft/sec, 7 blades, 3 flight conditions.

Figures 11a-11c. Broadband (bb) and thickness and loading (t+l) noise by design (i.e., tip speed/number of blades), 3 flight conditions.

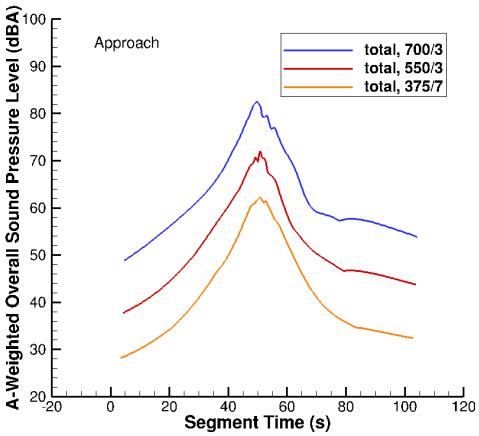

Figure 12a. Approach, 3 designs.

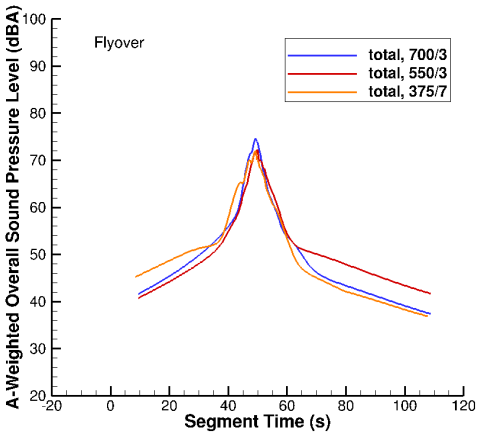

Figure 12b. Flyover, 3 designs.

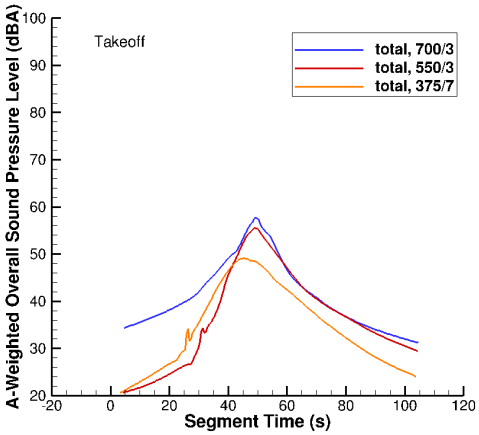

Figure 12c. Takeoff, 3 designs.

Figures 12a-12c. Total noise by flight condition, 3 designs (tip speed/number of blades). "700/3" denotes VTIP=700 ft/sec and 3 blades, for example.

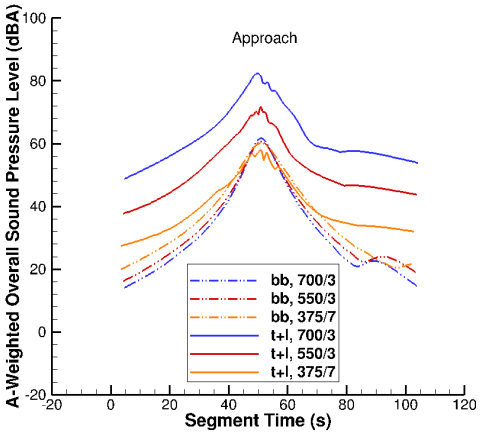

Figure 13a. Approach, 3 designs.

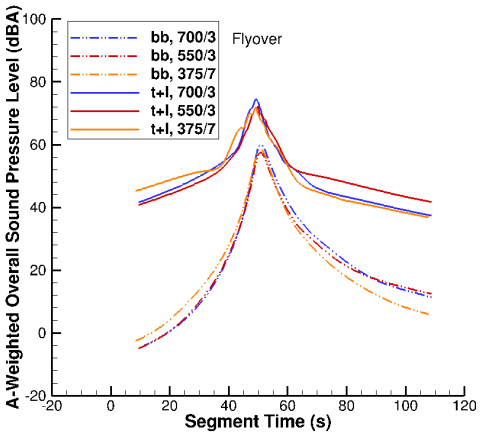

Figure 13b. Flyover, 3 designs.

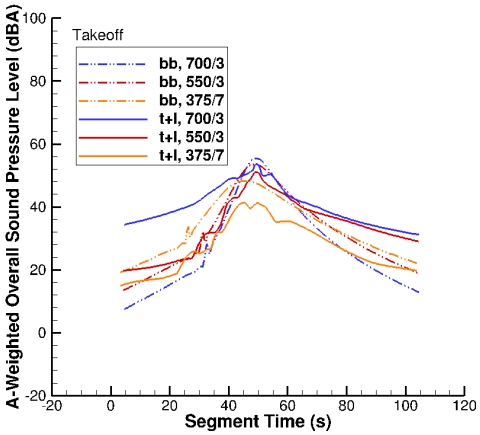

Figure 13c. Takeoff, 3 designs.

Figures 13a-13c. Broadband (bb) and thickness and loading (t+l) noise by flight condition, 3 designs (tip speed/number of blades). "700/3" denotes VTIP=700 ft/sec and 3 blades, for example.

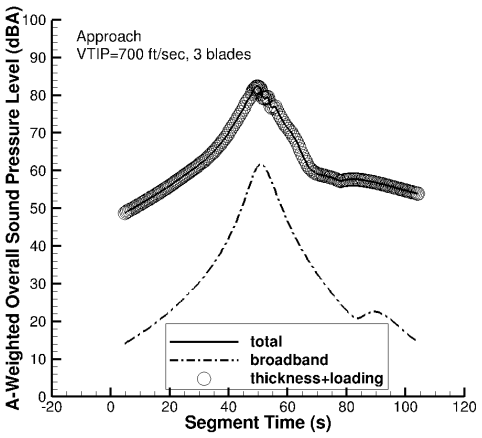

Figure 14a. Approach, VTIP=700 ft/sec, 3 blades.

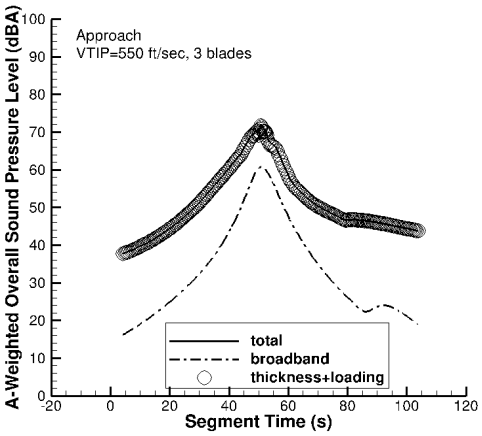

Figure 14b. Approach, VTIP=550 ft/sec, 3 blades.

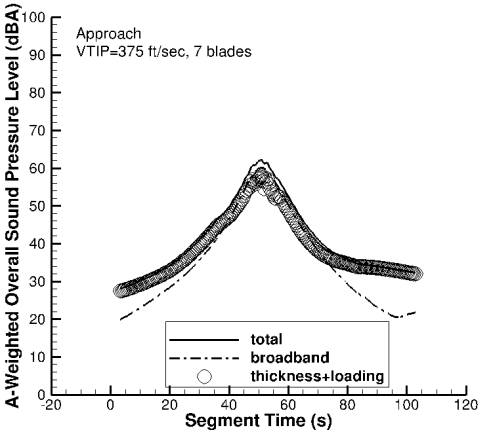

Figure 14c. Approach, VTIP=375 ft/sec, 7 blades

Figures 14a-14c. Approach – total, broadband, and thickness and loading noise, by design (tip speed/number of blades).

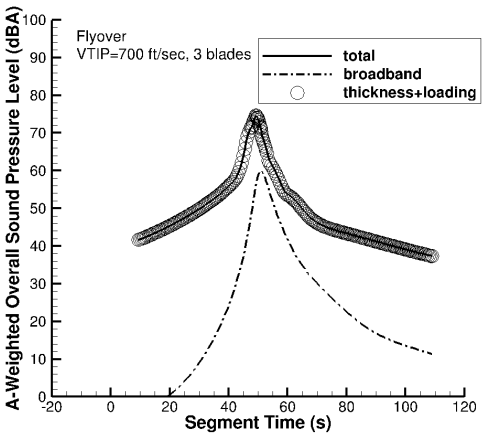

Figure 15a. Flyover, VTIP=700 ft/sec, 3 blades.

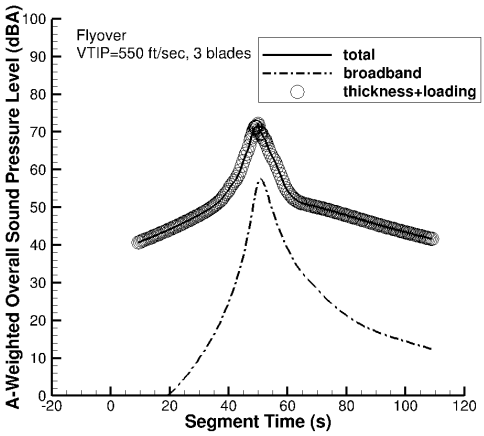

Figure 15b. Flyover, VTIP=550 ft/sec, 3 blades.

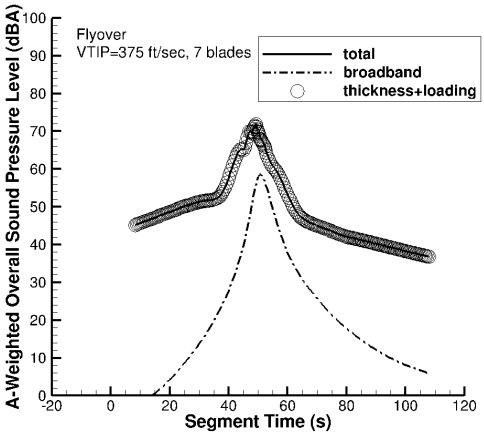

Figure 15c. Flyover, VTIP=375 ft/sec, 7 blades.

Figures 15a-15c. Flyover – total, broadband, and thickness and loading noise, by design (tip speed/number of blades).

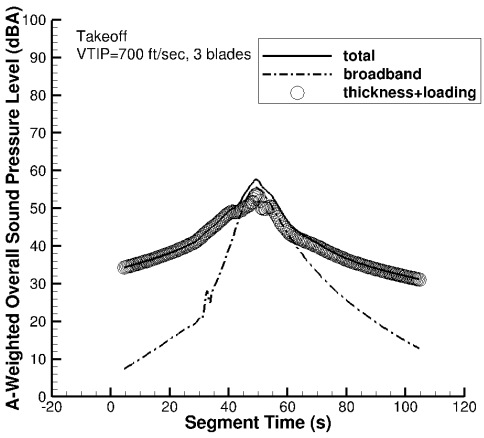

Figure 16a. Takeoff, VTIP=700 ft/sec, 3 blades.

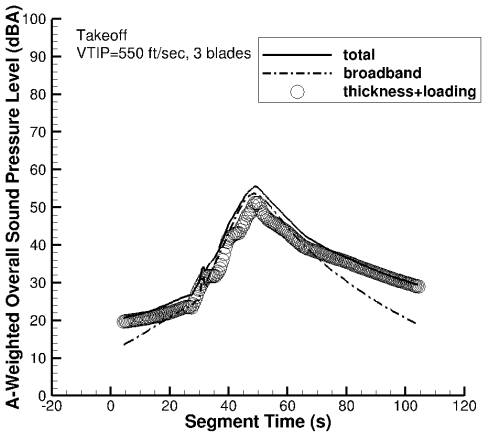

Figure 16b. Takeoff, VTIP=550 ft/sec, 3 blades.

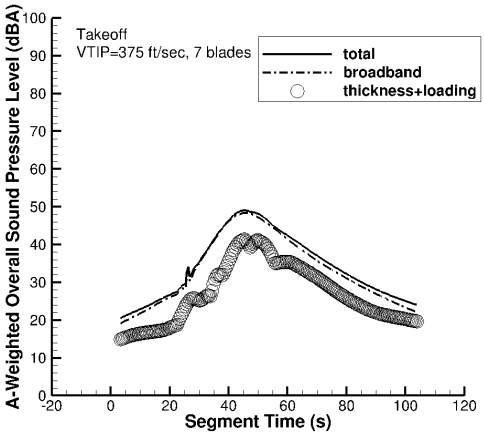

Figure 16c. Takeoff, VTIP=375 ft/sec, 7 blades.

Figures 16a-16c. Takeoff – total, broadband, and thickness and loading noise, by design (tip speed/number of blades).

Table 4. Approach, quadrotor A-weighted Lmax and EPNL (all four rotors, dB) – effect of lag hinge, nonuniformity, and elasticity, VTIP=550 ft/sec, 3 blades.

Noise source	1. Rigid uniform, flap/pitch	2. Rigid uniform, flap/lag/pitch	3. Rigid nonuniform, flap/lag/pitch	4. Elastic nonuniform, flap/lag/torsion
All sources	72.04	70.63	69.81	69.86
Thickness	21.45	21.89	21.87	22.44
Loading	**71.71**	**70.17**	**69.24**	**69.31**
Thickness + Loading	71.71	70.17	69.24	69.31
Self (Broadband)	60.72	60.72	60.69	60.66
EPNL	83.59	83.45	83.21	83.17
Loading noise difference	**0.00**	**-1.54**	**-2.47**	**-2.40**

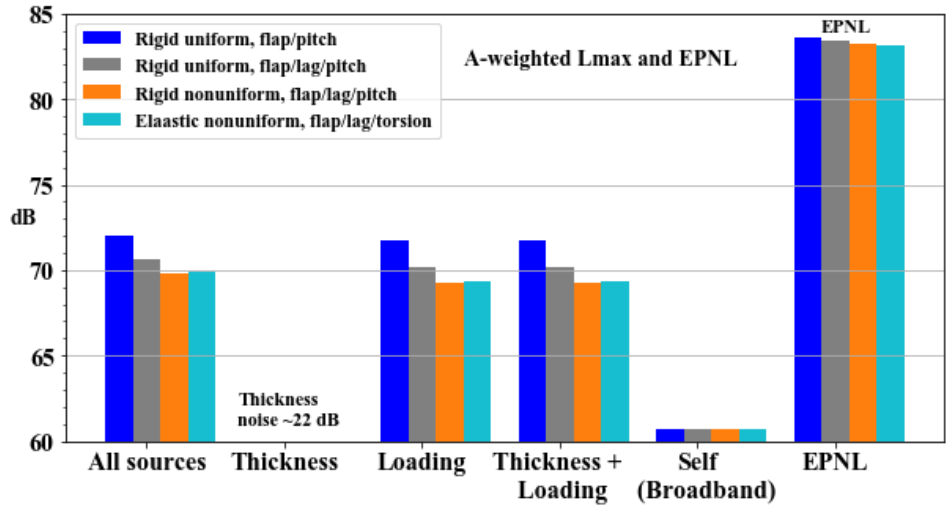

Figures 17. Approach, quadrotor A-weighted Lmax and EPNL (all four rotors) – effect of lag hinge, nonuniformity, and elasticity, VTIP=550/ft/sec, 3 blades.